Genetic Profile of Insertion Mutations in Mouse Leukemias and Lymphomas

Gwenn M. Hansen, Darlene Skapura and Monica J. Justice

Genome Res. 2000 10: 237-243
Access the most recent version at doi:10.1101/gr.10.2.237

Genetic Profile of Insertion Mutations in Mouse Leukemias and Lymphomas

Gwenn M. Hansen, Darlene Skapura, and Monica J. Justice[1]

Department of Molecular and Human Genetics, Baylor College of Medicine, One Baylor Plaza, Houston, Texas 77030 USA

Murine leukemia retroviruses (MuLVs) cause leukemia and lymphoma in susceptible strains of mice as a result of insertional mutation of cellular proto-oncogenes or tumor suppressor genes. Using a novel approach to amplify and sequence viral insertion sites, we have sequenced >200 viral insertion sites from which we identify >35 genes altered by viral insertion in four AKXD mouse strains. The class of genes most frequently altered are transcription factors, however, insertions are found near genes involved in signal transduction, cell cycle control, DNA repair, cell division, hematopoietic differentiation, and near many ESTs and novel loci. Many of these mutations identify genes that have not been implicated in cancer. By isolating nearly all the somatic viral insertion mutations contributing to disease in these strains we show that each AKXD strain displays a unique mutation profile, suggesting strain-specific susceptibility to mutations in particular genetic pathways.

AKXD recombinant inbred (RI) strains of mice develop a variety of hematopoietic cancers as a consequence of somatic viral insertions that alter the expression of cellular proto-oncogenes and tumor suppressor genes (Mucenski et al. 1986, 1987; Gilbert et al. 1993). Viral insertion site cloning within these strains has led to the identification of many proto-oncogenes as well as tumor suppressor genes, however, the majority of insertion mutations contributing to disease in these strains have not been identified, and few genes altered by viral insertion in B-cell leukemia have been cloned (van Lohuizen and Berns 1990).

Ideally, to determine the molecular genetic basis of leukemia and lymphoma, every somatic mutation contributing to disease should be identified. AKXD animals have proved to be extremely useful as genetic models of disease because affected genes are "tagged" by viral sequences. Unfortunately, current methods for identifying affected genes require the construction and screening of genomic libraries from individual tumor samples. Although effective, this approach is both time and labor intensive and has been the primary hindrance to identifying all virally induced somatic mutations. To avoid unnecessary cloning steps and speed identification of disease-causing mutations we used a novel approach to amplify and sequence viral insertion sites. This approach is based on a technique known as restriction-site PCR, which uses restriction enzyme (RE) recognition sequences as targets in unknown genomic DNA, enabling amplification between unknown genomic DNA and a known sequence. We used this technique to amplify genomic DNA-flanking murine proviral sequences. The viral insertion site amplification technique, or VISA, was used to screen tumors that arose in animals from AKXD RI mouse strains susceptible to B-cell leukemia and lymphoma. This screen identified the majority of virally induced somatic mutations within these tumors. Our approach greatly simplifies the effort needed to access cancer-causing mutations in the AKXD strains, providing an effective means for determining the molecular genetic basis of leukemia and lymphoma.

[1]Corresponding author.
E-MAIL mjustice@bcm.tmc.edu; FAX (713) 798-1489.

RESULTS

AKXD strains susceptible to B-cell leukemia or lymphoma (Mucenski et al. 1987; Gilbert et al 1993) were aged to collect tumors for analysis. Similar to previous studies, the AKXD mice showed strain-specific variation in their susceptibility to disease. The highest incidence of disease was observed in AKXD-18 animals, where 67% (42 of 63) developed either leukemia or lymphoma by 18 months of age. Animals from both the AKXD-13 and AKXD-27 strains showed moderate susceptibility, with 31% (18 of 58) and 55% (41 of 74) affected (respectively). In contrast, only 14% (4 of 29) of AKXD-10 animals developed disease.

To evaluate the VISA technique, tumors from these strains were screened using VISA to identify somatic viral insertion mutations (Fig. 1). A total of 217 genomic/proviral sequences were identified from screening 107 leukemias and lymphomas. These sequences represent 31 endogenous proviral elements and 186 somatic viral insertion site tags (VSTs). No VST sequences were identified from tumors that did not contain somatically acquired viruses detectable by Southern blot hybridization (data not shown). Database searches of the somatic VSTs identified 31 genes and expressed sequence tags (ESTs) in the nr-DNA and dbEST databases, several of which are known oncogenes or previously identified viral insertion sites (Table 1). Multiple VSTs representing independent in-

10:237–243 ©2000 by Cold Spring Harbor Laboratory Press ISSN 1054-9803/00 $5.00; www.genome.org

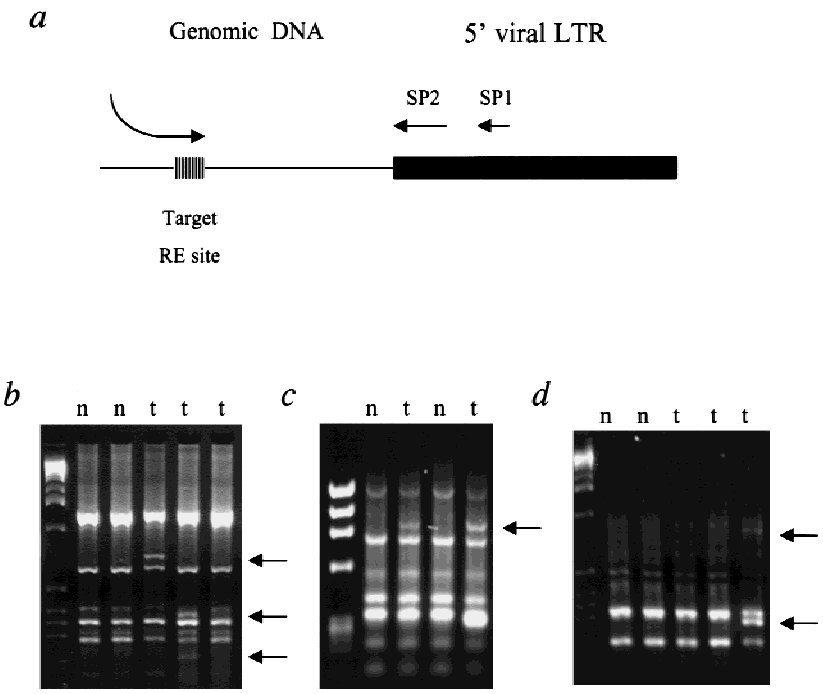

Figure 1 VISA PCR using MuLV LTR-specific primers. (*a*) Schematic representation of VISA. Viral insertion sites are amplified using primers specific for the long terminal repeat (LTR) of the MuLV in combination with RE-anchored degenerate primers that amplify from flanking genomic DNA. Two rounds of PCR are performed on unmodified genomic DNA using nested virus-specific primers to ensure specificity. Successful amplification of any viral insertion site is dependent on whether the RE anchor sequence is present in the genomic sequence flanking the viral LTR. Therefore, to increase the number of insertion mutations amplified, a minimum of five RE-anchored degenerate primers are used on each sample. The approximate binding sites for LTR specific primers SP1 and SP2 are shown. The RE-anchored degenerate primer contains an M13F linker (shown as a curved line) that is not expected to bind mouse DNA during the first round of PCR, but is useful for subsequent amplifications and sequencing. The stripped box indicates the location of the restriction enzyme recognition site target for the RE-anchored degenerate primer. (*b–d*) Representative examples of VISA products generated with RE-anchored primers specific for *Hin*dIII (*b*), *Eco*RI (*c*), and *Bcl*I (*d*). DNA isolated from brain tissue, which is rarely infiltrated by tumor cells, was used as a control to identify all nontarget amplification products such as endogenous proviral insertion sites, internal provirus sequences, or single primer amplification products generated by the restriction-site anchored primer. Tumor-specific VISA products, ranging in size from 50 bp to 2.0 Kb were gel purified and sequenced directly (identified by arrows). Lane designations are (n) (nontumor); (t) tumor.

sertion mutations at *Lvis1*, *Evi3*, and *Nmyc* were identified (Table 1). To determine whether VISA screening identified additional common insertion sites, the remaining set of VST sequences were compared with each other to determine whether multiple independent insertions occurred at the same genetic locus. These comparisons identified three new common sites of viral insertion, designated *Lvis2*, *Lvis3*, and *Lvis4*. Each of these loci were mapped by interspecific backcross to identify candidate genes. *Lvis2* cosegregates with marker *D7Mit237* on mouse chromosome 7 (Fig. 2a). No viral insertion sites have been mapped to this location; however, three genes are closely linked to this marker: stromal cell interacting factor 1 (*Stim1*), protein tyrosine phosphatase, nonreceptor type 5 (*Ptpn5*), and the SRY-box containing gene 6 (*Sox6*) (Mouse Genome Database 1999). Both *Sox6*, a transcription factor, and *Ptpn5*, a protein tyrosine phosphatase, have functions consistent with known oncogenes. *Stim1* is a stromal cell surface molecule identified for its ability to promote the survival or proliferation of pre-B cells in culture (Oritani and Kincade 1996). Although little additional information regarding *Stim1* function is available, the expression and proposed function for *Stim1* make it an interesting candidate disease gene. *Lvis3* cosegregates with markers on chromosome 13 and is tightly linked to the *Fim1* locus (Fig. 2b). *Fim1* is a common site of viral insertion in myeloblastic leukemias for which the affected gene has not yet been identified (Sola et al. 1986). Comparisons of restriction map data from *Fim1* and *Lvis3* indicate that these loci do not overlap (data not shown); however, further studies will be necessary to determine whether viral insertions at *Lvis3* and *Fim1* affect the same gene. *Lvis4* maps to distal chromosome 12, near the homeobox transcription factor *goosecoid*, and the T-cell leukemia translocation breakpoint *TCL1* (Virgilio et al. 1994; Mouse Genome Database 1999).

VISA screening identified 186 insertion mutations from 107 tumors. To estimate the percentage of total insertion mutations identified in the current study, Southern blot hybridizations were performed using probes for selected loci. Screening at *Evi3*, *Lvis1*, *Hex*, *Alx4*, and *Rel* detected proviral insertions in addition to those identified by VISA, whereas no additional alterations were identified using probes for *RecQ5* or *Erp72* (Table 1). These screens identified a total of 26 insertions, 17 of which were amplified and sequenced using VISA (65%). This is consistent with previous studies, which have indicated that most AKXD leukemias and lymphomas contain three to four somatic viral insertions (Mucenski et al. 1988; Gilbert et al. 1993), and suggests that although the majority of mutations have been identified, additional screening with degenerate primers targeting other restriction enzyme sequences will be necessary to identify all mutations.

The frequency of insertions at many of these loci varied significantly between AKXD strains. Although

Table 1. Sequence Identity of Loci Disrupted by Viral Insertion

Tumor	Common site	Candidate gene(s)[a]	Position[b]	Protein product	Type[c]	VST ID[d]
18-18	*Lvis1*	*Hex, Eg5*	IG	homeobox transcription factor (*Hex*),	B	18018G1
18-28	*Lvis1*		IG	kinesin-related spindle protein (*Eg5*)	T	18028G1
18-95	*Lvis1*		IG		B	18095G2
18-132	*Lvis1*		IG		B	18132G1
13-16	*Lvis1*		IG		B	13016G1
13-107	*Lvis1*		IG		B	13107G1
18-153	*Lvis1*		IG		B/T	18153G1
18-91	*Lvis1*		IG		B	S
27-28	*Lvis1*		IG		B	S
27-193	*Lvis1*		IG		B	S
27-16	*Evi3*	*Evi3*	UN	unknown	B	27016G2
27-57	*Evi3*		UN		B	27057G8
27-183	*Evi3*		UN		B	27183G3
27-205	*Evi3*		UN		B	27205G8
27-207	*Evi3*		UN		S	27207G1
27-258	*Evi3*		UN		B	27258G3
27-222	*Evi3*		UN		B	S
27-172	*Evi3*		UN		B	S
18-49	*N-myc*	*N-myc*	5′ E	nuclear protein	B/T	18049G1
18-109	*N-myc*		5′ E		B/T	18109G1
27-215	*N-myc*		3′ UTR		T	27215G1
18-60	*Lvis2*	unknown	UN	unknown	S	18060G6
18-67	*Lvis2*		UN		S	18067G2
27-110	*Lvis2*		UN		T	27110G1
18-72	*Lvis3*	unknown	UN	unknown	B	18072G2
18-132	*Lvis3*		UN		B	18132G2
10-60	*Lvis4*	unknown	UN	unknown	B/T	10060G2
27-266	*Lvis4*		UN		B	27266G1
18-34	*Lvis5*	*Alx4*	P	paired-type homeobox transcription factor	T	18034G2
27-110	*Lvis5*		UN		T	S
27-189	*Lvis7*	*Rel*	5′	transcription factor	B	27189G3
27-17	*Lvis7*		UN		S	S
27-129	*Lvis6*	*Hex*	3′ UTR	homeobox transcription factor	S	S
27-268	*Lvis6*		3′ UTR		B/T	S
27-28	*Lvis8*[e]	*CcnD3*	C	D cyclin	B	27028C5
27-178	*Lvis9*[e]	*Sox4*	3′ UTR	HMG-box transcription factor	B	27178G1
27-94	*Gfi1*	*Gfi1*	3′ UTR	zinc finger transcription factor	T	27094G3
18-123	*Myc*	*Myc*	P	nuclear protein	B/T	18123G2
13-23	*Notch1*	*Notch1*	3′ UTR	cell surface receptor	T	13023G1
27-16		*N-ras*	5′	GTP-binding protein	B	27016G1
27-107		*Cd5*	5′	cell surface receptor	S	27107C1
27-3		*Erp72*	P	endoplasmic reticulum protein	B	27003C4
18-33		*IgH*	3′ E	B-cell surface receptor	B/T	18033G3
10-11		*Mzfp2-related*	C	zinc finger transcription factor	B	10011C3
27-28		*RecQ5*	C	DNA helicase	B	27028C2
18-97		*Sip1*	3′ UTR	spliceosomal snRNP biogenesis	S	18097G2
27-30		18S rRNA	intron	rRNA	B	27030G1
18-43		U96726	IG	putative phosphoinositide 5-phosphatase type II	B	18043G4
27-28		AI250289		NCI CGAP Lym 12 follicular lymphoma EST	B	27028E1
27-3		N22410		EST	B	27003E5
18-123		AI549667		EST	B/T	18123E1
27-258		AA611619		EST	B	27258E2
27-3		AA546050		EST	B	27003E2
27-24		AI059755		EST	T	27024E2
13-36		AA636183		EST	B	13036E1
13-87		AA207479		EST	T	13087E1
13-44		AI644018		EST	N.D.	13044E1
13-53		AI615534		EST	B	13053E1
13-45		AA990077		EST	S	13045E1
13-37		AA1614004		EST	B	13037E1

Viral insertion sites identified using VISA or conventional Southern analysis are listed, except sites for which genes have not been identified (135 VSTs), or those representing endogenous insertion sites. All VISA products represent sequence 5′ of the proviral element (except *Evi3* tags, which are 3′ insertion sites), such that each insertion is identified only once.

[a]GenBank accession nos. are given for ESTs and genomic sequence contigs.

[b]Location of inserted viral element in relation to candidate gene as determined by Blast sequence alignment. [(C) coding; (E) enhancer; (IG) intergenic; (P) promoter; (UN) unknown; (UTR) untranslated region].

[c]Tumor cell type was determined by Southern analysis [(B) B cell; (T) T cell; (B/T) mixture of B and T cell; (S) progenitor or myeloid; (N.D.) not determined].

[d]Sequences have been deposited in GenBank, but can also be accessed at http://www.mouse-genome.bcm.tmc.edu/. [(S) insertion sites identified by conventional Southern analysis].

[e]Viral insertions at this locus were identified in other tumor subsets, indicating that this is a common site.

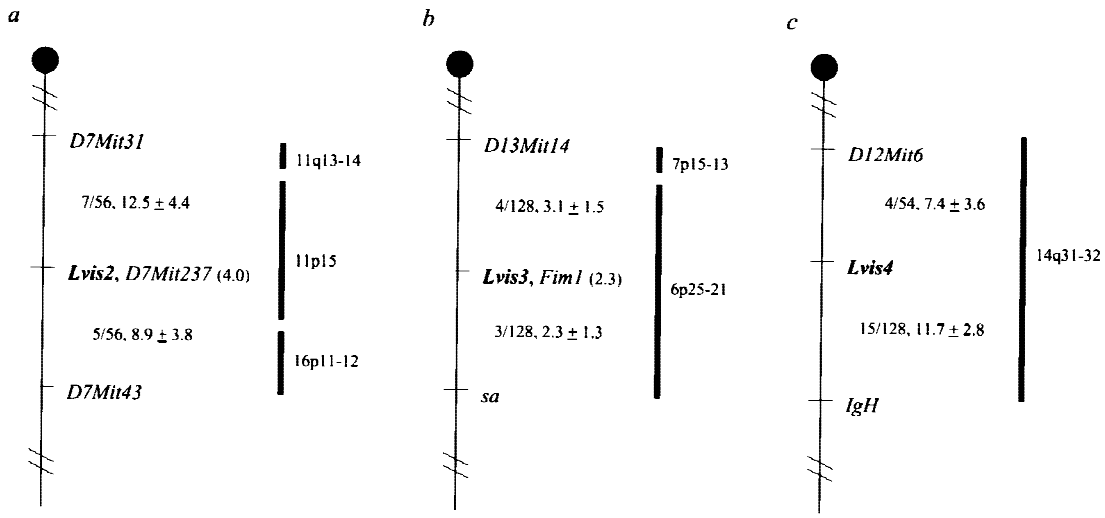

Figure 2 Meiotic mapping of *Lvis2–Lvis4*. *Lvis* viral insertion sites were mapped using an (SB/Le × *M. spretus*) F_1 × SB/Le interspecific backcross previously typed for multiple markers on all mouse chromosomes (Justice et al. 1990). Partial linkage maps of chromosomes 7 (*a*), 13 (*b*), and 12 (*c*) are depicted. Ratios of the total number of mice exhibiting recombinant chromosomes to the total number of mice analyzed for each pair of loci (with map distances in centimorgans ± the standard error) are shown to the left of each chromosome. For markers that cosegregate, the upper 95% confidence interval is shown in parentheses. The predicted map locations of human orthologs are indicated to the right of each chromosome. References and additional information regarding human map locations can be obtained from the Mouse Genome Database (http://www.informatics.jax.org/).

insertions at several loci such as *Evi3*, *Lvis3*, and *c-Rel* are strainspecific, insertions at *Alx4*, *Lvis1*, *Lvis2*, and *Lvis4* were observed in multiple strains (Table 2). In addition, several insertion mutations show tumor cell-type specificity, occurring primarily in B-lineage tumors (*Evi3*, *Lvis1*, *Lvis3*) or T-lineage tumors (*Alx4*). Notably, insertions at *Evi3* and *Lvis1* occur frequently in these strains, and likely play a significant role in B-cell disease.

DISCUSSION

The majority of virally induced somatic mutations in

Table 2. Strain-Specific Mutation Profile

Common site	Gene	Map location[a]	Insertion frequency (%)[b]			
			AKXD-10	AKXD13	AKXD-18	AKXD-27
Lvis1	*Hex, Eg5*	19 (26)[c]	0	11	14	5
Lvis2	unknown	7[c]	0	0	5	2
Lvis3	unknown	13[c]	0	0	5	0
Lvis4	unknown	12[c]	1/4	0	0	2
Lvis5	*Alx4*	2 (65)	0	0	2	2
Lvis6	*Hex*	19 (26)[c]	0	0	0	5
Lvis7	*Rel*	11 (13)	0	0	0	5
Lvis8	*CcnD3*	17	0	0	0	2
Lvis9	*Sox4*	13	0	0	0	2
Evi3	*Evi3*	18 (5)[c]	0	0	0	20
N-myc	*N-myc*	12 (4)	0	0	5	2
Gfi1	*Gfi1*	5 (56)	0	0	0	2
Myc	*Myc*	15 (32)	0	0	2	0
Notch1	*Notch1*	2 (15)	0	6	0	0

[a]Mouse chromosomal map locations either were determined in our laboratory or are based on published data. Primary mapping data are available from the Mouse Genome Informatics database (http://informatics.jax.org). Numbers in parentheses represent estimated distance from the centromere in centimorgans as assigned by MGD.
[b]Insertion frequency is calculated from a total of 18 AKXD-13 tumors, 42 AKXD-18 tumors and 41 AKXD-27 tumors, where the AKXD-10 frequency is shown as a fraction due to the number of tumors analyzed (4).
[c]Map locations determined using an (SB/Le × *M. spretus*)F_1 × SB/Le interspecific backcross (Justice et al. 1990).

primary leukemias and lymphomas from four AKXD strains were identified by direct amplification and sequencing using VISA. Viral insertions were identified at the common insertion sites *Evi3*, *Lvis1*, *Gfi1*, *Myc*, *Notch1*, and *Nmyc*, at eight new common insertion sites, *Lvis2–Lvis9*, and at many other genes and ESTs not previously implicated in cancer.

Multiple insertions were identified at *Lvis1*, the most frequently altered locus in AKXD B-cell neoplasias (Hansen and Justice 1999). Viral insertions at this site activate the expression of two distant genes, *Eg5* and *Hex* (Hansen and Justice 1999). EG5 is a kinesin-related spindle protein necessary for spindle assembly and cell division. The role of kinesin-related proteins in cancer is unclear; however, direct inhibition of *Eg5* has been shown to block mitosis by inhibiting bipolar spindle formation (Mayer et al. 1999). *Hex* is a divergent homeobox gene implicated in hematopoietic differentiation and transcriptional repression (Manfioletti et al. 1995; Tanaka et al. 1999). Homeobox genes and related transcription factors play a significant role in leukemia and lymphoma (Look 1997). In addition to insertions at *Lvis1*, insertions at *Lvis6* identify a common viral insertion site near the 3′ UTR of *Hex* in AKXD-27 tumors, providing additional evidence for the role of *Hex* in B-cell disease.

Multiple viral insertions were identified at *Lvis5*, a common site of viral insertion in the promoter region of the homeobox transcription factor *Alx4*. This gene contains a single paired-type DNA binding domain similar to the *Drosophila* "aristaless" protein (Qu et al. 1997). In the mouse, *Alx4* is expressed during early embryogenesis but is not expressed in later stages of development or in adult tissues (Qu et al. 1997). Mutations in *Alx4* produce preaxial polydactyly as well as a variety of other skeletal defects (Qu et al. 1998). The somatic mutations identified in this study provide the first evidence linking *Alx4* to cancer.

The common insertion site *Lvis7* identifies the *Rel* oncogene, belonging to the REL/NF-κB/IκB superfamily of signal transducers and transcription factors that carry out diverse functions in the immune system. *Rel* was initially identified as the mammalian homolog of the viral oncogene v-REL, which has been shown to promote cellular transformation both in vitro and in vivo (Sylla and Temin 1986; Moore and Bose 1988; Foo and Nolan 1999). Current studies suggest that the mechanism through which *Rel* and other family members mediate cellular transformation involves inappropriate protection or rescue from apoptotic signals (Foo and Nolan 1999). Notably, although *Rel* has been implicated in lymphoma development, our study is the first to identify it as a common viral insertion site, demonstrating the efficacy of the VST technique for identifying cancer-causing genes.

Many of the known AKXD disease genes were identified using VISA. However, insertions near *Pim1*, *Evi1*, *Fis1*, and *Pvt1*, which have been observed in AKXD tumors (Mucenski et al. 1987, 1988), were not identified in this study. Insertion mutations at these sites occur infrequently in the four AKXD strains screened by VISA; therefore, it is possible that insertions at these sites do not occur in this tumor subset. Alternatively, although we have isolated the majority of insertion mutations, additional screening may be necessary to identify all genes altered. It is also important to note that previous studies used Southern blot hybridization to screen several kilobases of genomic DNA at each locus, little of which is represented in current sequence databases. This is certainly the case for *Fis1*, where no sequence data is available.

A large number of the viral insertion site sequences did not show similarity to each other or to sequences in available databases (135 of 186, or 73%). These insertions may lie at a distance from candidate genes, or may occur within introns or near 5′ or 3′ regulatory elements for which sequence is not available. Alternatively, they may identify novel genes. Several VSTs showed similarity to mouse, human, and rat ESTs, one of which is a CGAP EST expressed in human follicular lymphoma (Table 1). Cross-referencing mutation and sequence databases such as these is likely to reveal roles for many novel genes. Identification of candidate genes for the remaining VSTs is essential for a complete understanding of hematopoietic diseases, and will require forthcoming genomic sequence information from mouse and human genome sequencing efforts (Collin et al. 1998; Battey et al. 1999).

For sites where genes can be immediately identified, it is clear that many have the potential to contribute to the disease process. Insertions near *CcnD3*, *Gfi1*, *Myc*, *Notch1*, *Nras*, and *Sox4* were each observed once. These genes have been identified as cellular proto-oncogenes or common viral insertion sites in other tumor subsets or model systems (Corcoran et al. 1984; Gilks et al. 1993; Steffen 1984). Obviously none of these loci play a significant role overall in the disease process observed in these AKXD strains. Nonetheless, a viral insertion mutation near any one of these genes would likely provide a growth advantage to the individual tumor in which it occurred. Certainly any of the genes identified near viral insertion sites could contribute to disease. One gene of particular interest is *RecQ5*. RecQ helicases function in DNA repair, recombination, and replication. Mutations in three of the five human RecQ proteins are associated with diseases involving predisposition to malignancies and increased chromosomal instability (Ellis et al. 1995; Yu et al. 1996; Kitao et al. 1999). Recent mapping of *RecQ5* has localized this gene to human chromosome 17q23–25, a region associated with both breast and ovarian cancer (Sekelsky et al. 1999). Our data identify *RecQ5* as a potential proto-

oncogene in mouse leukemia, and suggest that further study of *RecQ5* in cancer is warranted.

In addition to implicating multiple loci in hematopoietic disease, analysis of VSTs revealed distinct mutation profiles within AKXD strains. This implies that although a variety of genes can contribute to malignant transformation, susceptibility alleles within each genetic background determine mutation oncogenicity. Although further work will be necessary to identify these susceptibility alleles, the VSTs represent the majority of genes that contribute to disease onset and progression within the hematopoietic lineages of these strains. These data can be integrated with both genomic and gene expression profiles from human cancers to uncover the pathways involved in the development of leukemia and lymphoma in both mouse and human.

METHODS

Mice

Mice from four AKXD strains, AKXD-10, AKXD-13, AKXD-18, and AKXD-27, were obtained from The Jackson Laboratory and maintained in our colony at Oak Ridge National Laboratory. Animals were monitored weekly for signs of illness, and moribund animals or healthy animals reaching the age of 18 months were autopsied and evaluated for signs of lymphoma. Normal and affected tissues were snap-frozen in liquid nitrogen.

DNA Extraction

High molecular weight DNA was isolated from tumor-infiltrated and normal tissues as described (Wu et al. 1995), followed by a single phenol/chloroform extraction and ethanol precipitation following standard procedures (Sambrook et al. 1989).

Overview of VISA

Mouse genomic sequence flanking inserted proviral elements was amplified using two rounds of PCR. The initial PCR was performed on 200 ng of genomic DNA using a restriction site-anchored degenerate primer (Sarkar et al. 1993) and a MuLV long terminal repeat (LTR)-specific primer (SP1). The second round PCR was performed using 1 µl of first round reaction as template, with a nested LTR-specific primer (SP2) and the M13F primer, which is included as an adapter in the degenerate primer design. Second-round PCR products were separated by gel electrophoresis, and tumor-specific VISA products were purified and sequenced (Fig. 1).

Oligonucleotide Primers

Nested primers specific to the ecotropic MuLV LTR were designed to amplify the upstream insertion junction. These primers (first round) SP1 5′-CTGAGAACATCAGCTCTG-3′ and (second round) SP2 5′-CTGGCTAAGCCTTATGAAGGGGTCTTTC-3′ bind 70 bp and 1 bp from the 5′ LTR terminus, respectively. To amplify sequences downstream of the proviral element, primers (first round) 5′-AATCAGCTCGCTTCTCGC-3′ and (second round) 5′-GAGGGTCTCCTCAGAGTGATTGACTGC-3′ were used, binding 223 bp and 21 bp from the 3′ LTR terminus, respectively. The degenerate primer design consisted of three regions: an anchor sequence of four to six nucleotides based on RE recognition sequences, a fully degenerate region of eight nucleotides, and an adapter region consisting of the M13F primer sequence (for example, to target the restriction enzyme recognition sequence *Eco*RI, 5′-GGGTTTTCCCAGTCACGACNNNNNNNNGAATTC-3′). Primers targeting *Eag*I, *Eco*RI, *Hin*dIII, *Sac*I, and *Xba*I were used on all tumor samples. Additional screens using primers for *Bcl*I, *Bss*HII, *Pst*I, *Sac*II, or *Taq*I were performed on those samples not generating products after the initial screen.

PCR Conditions

PCR was performed using a MJ Research thermal controller with the cycling parameters: 94°C for 3 min, 30 cycles of 94°C for 30 sec, 50°C for 2 min, and 72°C for 2 min, with a final 7-min incubation at 72°C. The initial round of PCR contained 200 ng of genomic DNA, 2.5 pmoles of SP1, 25 pmoles of degenerate primer, 1.5 mM MgCl, 0.2 mM each dNTP, 2.5 µl 10× PCR buffer, 1 M betaine, and 0.25 µl *Taq* DNA polymerase in a volume of 25 µl. One microliter of this reaction was used as template in a nested reaction with the following changes: 25 pmoles of both SP2 and M13F were used as primers, and the annealing temperature was increased to 55°C. Each reaction was electrophoresed on a 2% SeaPlaque GTG agarose gel in 1× TAE. Products of interest were purified using the QIAquick gel extraction kit (Qiagen) and sequenced using the M13F and SP2 primers.

DNA Sequencing and Analysis

DNA was sequenced using the ABI Prism BigDye Terminator Cycle Sequencing Kit (Perkin Elmer) on an ABI model 377 DNA Sequencer (Applied Biosystems). Sequence files were edited to remove ambiguous bases and were analyzed for sequence overlap using Sequencher (Gene Codes Corporation Inc.). Sequence from each product was verified to contain the target RE sequence and viral LTR sequence. Sequences representing endogenous proviral elements were identified by comparison with sequenced products amplified from nontumor DNA. In cases were a single insertion mutation was amplified more than once by different RE-anchored degenerate primers, only the largest sequence was used. Edited sequence files were searched against available sequence databases using the gapped BLAST algorithms BLAST-nr, BLASTN-dbEST, and BLASTX-nr (Gish and States 1993; Altschul et al. 1997).

Genetic Mapping

Loci were mapped using an (SB/Le × *M. spretus*) F_1 × SB/Le interspecific backcross previously typed for multiple markers on all mouse chromosomes (Justice et al. 1990). Informative restriction fragment length polymorphisms were monitored in 130 N_2 progeny to determine linkage. Additional information regarding allele sizes and informative polymorphisms has been deposited in the Mouse Genome Database (http://www.informatics.jax.org).

Southern Blot Analysis

Membranes were prehybridized and hybridized as described (Church and Gilbert 1984). Probes for IgH, Igκ, Jβ1, and Jβ2 have been described (Kronenberg et al. 1985; Mucenski et al. 1986). Probes representing *Lvis1*, the 3′ UTR of the *Hex* gene, and the *Evi3* insertion site have been described (Justice 1994; Hansen and Justice 1999). All other probes were derived from VISA PCR products. Probes were radioactively labeled using the Prime-It kit (Stratagene).

Classification of Tumors

Tumors were classified as B, T, or mixed lineage based on BCR (IgH and Igκ) or TCR (Jβ1 or Jβ2) gene rearrangements. Tumors showing no BCR or TCR gene rearrangements may represent either progenitor or myeloid tumors (Mucenski et al. 1988).

ACKNOWLEDGMENTS

We thank Toni Jago for assistance in tissue collection. This work is supported by a grant from the National Cancer Institute (R29CA63229), and by an American Cancer Society Junior Faculty Research Award (JFRA0553) to M.J.J.

The publication costs of this article were defrayed in part by payment of page charges. This article must therefore be hereby marked "advertisement" in accordance with 18 USC section 1734 solely to indicate this fact.

REFERENCES

Altschul, S., T. Madden, A. Schaffer, J. Zhang, Z. Zhang, W. Miller, and D. Lipman. 1997. Gapped BLAST and PSI-BLAST: A new generation of protein database search programs. *Nucleic Acids Res.* **25:** 3389–3402.

Battey, J., E. Jordan, D. Cox, and W. Dove. 1999. An action plan for mouse genomics. *Nature Genet.* **21:** 73–75.

Church, G. and W. Gilbert. 1984. Genomic sequencing. *Proc. Natl. Acad. Sci.* **81:** 1991–1995.

Collins, F., A. Patrinos, E. Jordan, A. Chakravarti, R. Gesteland, and L. Walters. 1998. New goals for the U.S. Human Genome Project: 1998–2003. *Science* **282:** 682–689.

Corcoran, L., J. Adams, A. Dunn, and S. Cory. 1984. Murine T lymphomas in which the cellular myc oncogene has been activated by retroviral insertion. *Cell* **37:** 113–122.

Ellis, N., J. Groden, T. Ye, J. Straughen, D. Lennon, S. Ciocci, M. Proytcheva, and J. German. 1995. The Bloom's syndrome gene product is homologous to RecQ helicases. *Cell* **83:** 655–666.

Foo, S. and G. Nolan. 1999. NF-kappaB to the rescue: RELs, apoptosis and cellular transformation. *Trends Genet.* **15:** 229–235.

Gilbert, D., P. Neumann, B. Taylor, N. Jenkins, and N. Copeland. 1993. Susceptibility of AKXD recombinant inbred mouse strains to lymphomas. *J. Virol.* **67:** 2083–2090.

Gilks, C., S. Bear, H. Grimes, and P. Tsichlis. 1993. Progression of interleukin-2 (IL-2)-dependent rat T cell lymphoma lines to IL-2-independent growth following activation of a gene (Gfi-1) encoding a novel zinc finger protein. *Mol. Cell. Biol.* **13:** 1759–1768.

Gish, W. and D. States. 1993. Identification of protein coding regions by database similarity search. *Nature Genet.* **3:** 266–272.

Hansen, G.M. and M.J. Justice. 1999. Activation of Hex and mEg5 by retroviral insertion may contribute to mouse B-cell leukemia. *Oncogene* **18:** 6531–6539.

Justice, M., C. Silan, J. Ceci, A. Buchberg, N. Copeland, and N. Jenkins. 1990. A molecular genetic linkage map of mouse chromosome 13 anchored by the beige (bg) and satin (sa) loci. *Genomics* **6:** 341–351.

Justice, M., H.R. Morse, N. Jenkins, and N. Copeland. 1994. Identification of Evi-3, a novel common site of retroviral integration in mouse AKXD B-cell lymphomas. *J. Virol.* **68:** 1293–1300.

Kitao, S., A. Shimamoto, M. Goto, R. Miller, W. Smithson, N. Lindor, and Y. Furuichi. 1999. Mutations in RECQL4 cause a subset of cases of Rothmund-Thomson syndrome. *Nature Genet.* **22:** 82–84.

Kronenberg, M., J. Goverman, R. Haars, M. Malissen, E. Kraig, L. Phillips, T. Delovitch, N. Suciu-Foca, and L. Hood. 1985. Rearrangement and transcription of the beta-chain genes of the T-cell antigen receptor in different types of murine lymphocytes. *Nature* **313:** 647–653.

Look, A. 1997. Oncogenic transcription factors in the human acute leukemias. *Science* **278:** 1059–1064.

Manfioletti, G., V. Gattei, E. Buratti, A. Rustighi, A. De Iuliis, D. Aldinucci, G. Goodwin, and A. Pinto. 1995. Differential expression of a novel proline-rich homeobox gene (Prh) in human hematolymphopoietic cells. *Blood* **85:** 1237–1245.

Mayer, T., T. Kapoor, S. Haggarty, R. King, S. Schreiber, and T. Mitchison. 1999. Small molecule inhibitor of mitotic spindle bipolarity identified in a phenotype-based screen. *Science* **286:** 971–974.

Mouse Genome Database (MGD). *Mouse Genome Informatics*. The Jackson Laboratory, Bar Harbor, Maine 1999. World Wide Web (URL: http://www.informatics.jax.org/).

Moore, B. and H.J. Bose. 1988. Transformation of avian lymphoid cells by reticuloendotheliosis virus. *Mutat. Res.* **195:** 75–90.

Mucenski, M., B. Taylor, N. Jenkins, and N. Copeland. 1986. AKXD recombinant inbred strains: models for studying the molecular genetic basis of murine lymphomas. *Mol. Cell. Biol.* **6:** 4236–4243.

Mucenski, M., D. Gilbert, B. Taylor, N. Jenkins, and N. Copeland. 1987. Common sites of viral integration in lymphomas arising in AKXD recombinant inbred mouse strains. *Oncogene Res.* **2:** 33–48.

Mucenski, M., B. Taylor, J. Ihle, J. Hartley, H.C. Morse III, N. Jenkins, and N. Copeland. 1988. Identification of a common ecotropic viral integration site, Evi-1, in the DNA of AKXD murine myeloid tumors. *Mol. Cell. Biol.* **8:** 301–308.

Oritani, K. and P.W. Kincade. 1996. Identification of stromal cell products that interact with pre-B cells. *J. Cell. Biol.* **134:** 771–782.

Qu, S., L. Li, and R. Wisdom. 1997. Alx-4: cNDA cloning and characterization of a novel paired-type homeodomain protein. *Gene* **203:** 217–223.

Qu, S., S. Tucker, J. Ehrlich, J. Levorse, L. Flaherty, R. Wisdom, and T. Vogt. 1998. Mutations in mouse Aristaless-like4 cause Strong's luxoid polydactyly. *Development* **125:** 2711–2721.

Sambrook, J., E. Fritsch, and T. Maniatis. 1989. *Molecular cloning: A laboratory manual*, 2nd ed. Cold Spring Harbor Laboratory Press, Cold Spring Harbor, NY.

Sarkar, G., R. Turner, and M. Bolander. 1993. Restriction-site PCR: A direct method of unknown sequence retrieval adjacent to a known locus by using universal primers. *PCR Methods Appl.* **2:** 318–322.

Sekelsky, J., M. Brodsky, G. Rubin, and R. Hawley. 1999. Drosophila and human RecQ5 exist in different isoforms generated by alternative splicing. *Nucleic Acids Res.* **27:** 3762–3769.

Sola, B., S. Fichelson, D. Bordereaux, P. Tambourin, and S. Gisselbrecht. 1986. fim-1 and fim-2: Two new integration regions of Friend murine leukemia virus in myeloblastic leukemias. *J. Virol.* **60:** 718–725.

Steffen, D. 1984. Proviruses are adjacent to c-myc in some murine leukemia virus-induced lymphomas. *Proc. Natl. Acad. Sci.* **81:** 2097–2101.

Sylla, B. and H. Temin. 1986. Activation of oncogenicity of the c-rel proto-oncogene. *Mol. Cell. Biol.* **6:** 4709–4716.

Tanaka, T., T. Inazu, K. Yamada, Z. Myint, V. Keng, Y. Inoue, N. Taniguchi, and T. Noguchi. 1999. cDNA cloning and expression of rat homeobox gene, Hex, and functional characterization of the protein. *Biochem. J.* **339:** 111–117.

van Lohuizen, M. and A. Berns. 1990. Tumorigenesis by slow-transforming retroviruses—An update. *Biochim. Biophys. Acta.* **1032:** 213–235.

Virgilio, L., M. Narducci, M. Isobe, L. Billips, M. Cooper, C. Croce, and G. Russo. 1994. Identification of the TCL1 gene involved in T-cell malignancies. *Proc. Natl. Acad. Sci.* **91:** 12530–12534.

Wu, Q., M. Chen, M. Buchwald, and R. Phillips. 1995. A simple, rapid method for isolation of high quality genomic DNA from animal tissues. *Nucleic Acids Res.* **23:** 5087–5088.

Yu, C.-E., J. Oshima, Y. Fu, E. Wijsman, F. Hisama, R. Alisch, S. Matthews, J. Nakura, T. Miki, S. Ouais, G. Martin, J. Mulligan, and G. Schellenberg. 1996. Positional cloning of the Werner's syndrome gene. *Science* **272:** 258–262.

Received October 6, 1999; accepted in revised form December 9, 1999.